

REPORT

Unusual Thermal Stability of High-Entropy Alloy Amorphous Structure

Basic research for AOARD 114009

Award No. FA2386-11-1-4009

Principal Investigator: Professor Jien-Wei Yeh
Department of Materials Science and Engineering
National Tsing Hua University

Date: June 20, 2012

Report Documentation Page

Form Approved
OMB No. 0704-0188

Public reporting burden for the collection of information is estimated to average 1 hour per response, including the time for reviewing instructions, searching existing data sources, gathering and maintaining the data needed, and completing and reviewing the collection of information. Send comments regarding this burden estimate or any other aspect of this collection of information, including suggestions for reducing this burden, to Washington Headquarters Services, Directorate for Information Operations and Reports, 1215 Jefferson Davis Highway, Suite 1204, Arlington VA 22202-4302. Respondents should be aware that notwithstanding any other provision of law, no person shall be subject to a penalty for failing to comply with a collection of information if it does not display a currently valid OMB control number.

1. REPORT DATE 03 JUL 2012		2. REPORT TYPE Final		3. DATES COVERED 14-12-2010 to 13-11-2011	
4. TITLE AND SUBTITLE Unusual thermal stability of high-entropy alloy amorphous structure				5a. CONTRACT NUMBER FA23861114009	
				5b. GRANT NUMBER	
				5c. PROGRAM ELEMENT NUMBER	
6. AUTHOR(S) Jien-Wei Yeh				5d. PROJECT NUMBER	
				5e. TASK NUMBER	
				5f. WORK UNIT NUMBER	
7. PERFORMING ORGANIZATION NAME(S) AND ADDRESS(ES) National Tsing Hua University,101, Sec 2, Kuang-Fu Rd, Hsinchu,Taiwan 30043,Taiwan,NA,NA				8. PERFORMING ORGANIZATION REPORT NUMBER N/A	
9. SPONSORING/MONITORING AGENCY NAME(S) AND ADDRESS(ES) AOARD, UNIT 45002, APO, AP, 96338-5002				10. SPONSOR/MONITOR'S ACRONYM(S) AOARD	
				11. SPONSOR/MONITOR'S REPORT NUMBER(S) AOARD-114009	
12. DISTRIBUTION/AVAILABILITY STATEMENT Approved for public release; distribution unlimited					
13. SUPPLEMENTARY NOTES					
14. ABSTRACT NbSiTaTiZr alloy was designed to have two combined effects: high entropy effect and large atomic size effect which are intended to give unusual thermal stability of amorphous structure. The outcome is that the amorphous structure of deposited alloy film on sapphire substrate can be retained even annealed at 850 °C for at least 3 h. If substrate effect could be eliminated, the crystallization temperature would be higher.					
15. SUBJECT TERMS high entropy alloys					
16. SECURITY CLASSIFICATION OF:			17. LIMITATION OF ABSTRACT Same as Report (SAR)	18. NUMBER OF PAGES 17	19a. NAME OF RESPONSIBLE PERSON
a. REPORT unclassified	b. ABSTRACT unclassified	c. THIS PAGE unclassified			

Unusual Thermal Stability of High-Entropy Alloy Amorphous Structure

Chun-Yang Cheng^a, Wan-Jui Shen^a, and Jien-Wei Yeh^{a,*}

^aDepartment of Materials Science and Engineering, National Tsing Hua University,
Hsinchu 30013, Taiwan

*E- mail: jwyeh@mx.nthu.edu.tw; Telephone number: +886 3 5719558; Fax number:
+886 3 5722366

ABSTRACT

NbSiTaTiZr alloy was designed to have two combined effects: high entropy effect and large atomic size effect which are intended to give unusual thermal stability of amorphous structure. The outcome is that the amorphous structure of deposited alloy film on sapphire substrate can be retained even annealed at 850 °C for at least 3 h. If substrate effect could be eliminated, the crystallization temperature would be higher.

I. Introduction

Metallic glasses (MGs) with proper alloy design are fascinated with their unique and remarkable properties such as excellent mechanical properties (high strength), corrosion resistance and magnetic properties (soft and hard magnetism)^[1-15]. MGs accompanying with these outstanding features are promising for advanced applications; therefore, many researchers exert themselves on studying MGs^[16-19]. Various metallic glass systems as bulk forms, powders, and films and their fabrication processes have been widely studied and developed. Physical vapor deposition and mechanical alloying were applied in preparation of films and powders of MGs,

respectively^[5,6,11]. Rapid solidification techniques were utilized to manufacture metallic glass ribbons^[20]. With certain alloy compositions design, metallic glasses could be produce as bulk forms under moderate cooling rates due to their higher glass forming ability, which are often called bulk metallic glasses (BMGs) or bulk glassy alloys (BGAs)^[16,19]. In last three decades, bulk metallic glasses have been extensively investigated. Inoue *et al.*^[16,19] proposed three empirical rules for designing BMGs: (1) multi-component, consisting of three elements or more; (2) significant atomic size difference >12% among the three main constituent elements; and (3) negative heats of mixing among the three main elements. However, the recrystallization temperatures of reported BMGs are quite low, usually under 800 K^[4,21]. As recrystallization would eliminate the merits of amorphous structure, MGs and BMGs with higher recrystallization temperatures, i.e., having higher thermal stability in processing or applications, are always the important issue in their developments.

On the basis of above considerations, several multi-principal elements alloy systems of high-entropy alloys (HEAs), were designed and studied in order to enhance thermal stability of amorphous structure at high temperatures in our previous research. Within these studies, the high-entropy NbSiTaTiZr alloy film with amorphous phase possesses noteworthy thermal stability. It was found that this metallic glass film can maintain amorphous structure at 900 °C (1173 K) for several hours. This record is much higher than those recrystallization temperatures of MGs and BMGs reported^[4,21]. This study is thus intended to check this high thermal stability and understand its mechanism in consideration of the importance of outstanding high thermal stability behavior found in high-entropy alloy system.

II. Experimental procedures

The sputtering target of NbSiTaTiZr equal-mole high-entropy alloy used was prepared with Nb, Si, Ta, Ti, and Zr elemental raw materials via vacuum arc-melting in a water-cooled crucible. The melting and solidification were repeatedly for at least 5 times to ensure the chemical homogeneity. The solidified slab was then cut and polished into a disc 2 inch in diameter. Sapphire wafers were utilized as the substrate for the deposition of the alloy films from the NbSiTaTiZr target. The deposition method is DC magnetron sputtering operated at a target power of 150 W and under a base pressure better than 5×10^{-6} torr and a working pressure fixed at 5×10^{-3} torr with an argon gas flow of 20 sccm. The as-deposited specimens were subjected to rapid thermal annealing (RTA) at different temperatures from 300 °C to 900 °C for at least 1 h under high vacuum condition $< 5 \times 10^{-7}$ torr.

Chemical composition of NbSiTaTiZr alloy coatings were analyzed using an electron probe microanalyzer (EPMA, JEOL JAX-8800). The crystallographic structures of as-deposited and annealed metallic films were characterized utilizing a glancing incident angle X-ray diffractometer (GIAXRD, RIGAKU D/MAX2500) with Cu K α radiation and at the incident angle of 1°. The surface morphology and microstructures were observed with field-emission scanning electron microscope (FESEM, JOEL JSM 6500F). The structure evolutions of annealed NbSiTaTiZr alloy thin films were investigated with transmission electron microscope (JEM-2100F).

III. Results and Discussion

1. EPMA and XRD analyses on as-deposited and as-annealed films

The chemical compositions of as-deposited, 850 °C-annealed and 900 °C-annealed NbSiTaTiZr alloy thin films were analyzed by EPMA, as listed in Table 1. It confirms that compositions of NbSiTaTiZr alloy films under various states are very close to our equimolar design (20 at %).

Table 1. Actual compositions of thin films at various states compared with nominal composition designed

Content (at %)	Elements				
	Nb	Si	Ta	Ti	Zr
alloy design	20	20	20	20	20
as-deposited	20.2	19.1	21.3	19.5	19.9
850 °C annealed	21.0	20.1	20.4	18.3	20.2
900 °C annealed	19.9	19.5	22.6	18.6	19.5

Figure 1 shows the XRD patterns of NbSiTaTiZr alloy thin films under as-deposited state and as-annealed states after annealing at various temperatures between 300 °C and 900 °C for one hour. The as-deposited thin film possesses amorphous structure. All annealed samples except that annealed at 900 °C, exhibit single diffuse peak (range of $2\theta > 15^\circ$). It should be noted that the diffuse peaks of most annealed patterns are lower and broader than that of the as-deposited one. This implies that the annealing at higher temperatures render the amorphous structure more disordered, i.e., with higher degree of disorder, as the samples was fast cooled after annealing. This unusual trend as opposed to the general trend towards crystallization

suggests the existence of high entropy effect which tends to let the solution become more random at higher temperatures. However, the 900 °C-annealed one clearly illustrates the commencement of crystallization in this NbSiTaTiZr alloy thin film.

NbSiTaTiZr - Vacuum Annealing (1 h)

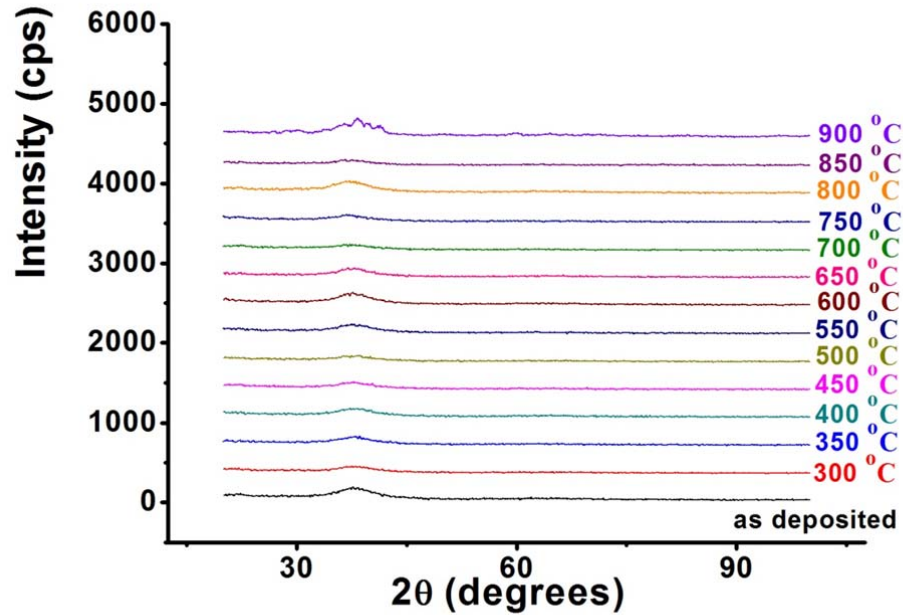
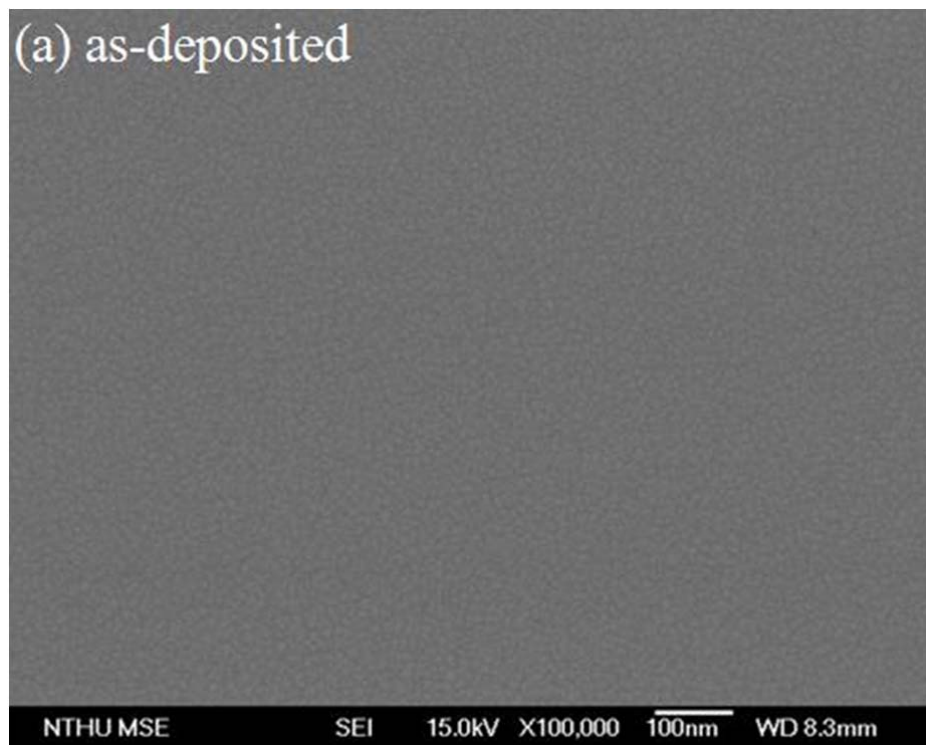


Figure 1. XRD patterns of NbSiTaTiZr alloy thin films under as-deposited state and as-annealed states after annealing at various temperatures between 300 °C and 900 °C for one hour.

2. FE-SEM investigations on as-deposited and as-annealed films

Figure 2(a), 2(b) and 2(c) show the FE-SEM images of as-deposited, 850 °C-annealed and 900 °C-annealed alloy thin films, respectively. It reveals that as-deposited film exhibits very uniform and smooth surface even seen under very high magnification. The very fine clusters are equiaxed and around 8 nm in size which are

the typical feature of amorphous film in which all clusters are amorphous. 850 °C-annealed film still displays similar features but clusters' contrast becomes poorer than that of as-deposited film. This suggests the smoothening effect during annealing which might due to the surface tension effect to minimize the surface area as seen in the fire polishing on glass surface. Nonetheless, 900 °C-annealed alloy film shows extra feature. There are a number of larger grains distributed randomly on the film surface. The average size of these grains is about 15 nm. Accompanying with the crystallization phenomenon revealed by XRD pattern, this suggests the larger grains are very probably crystalline.



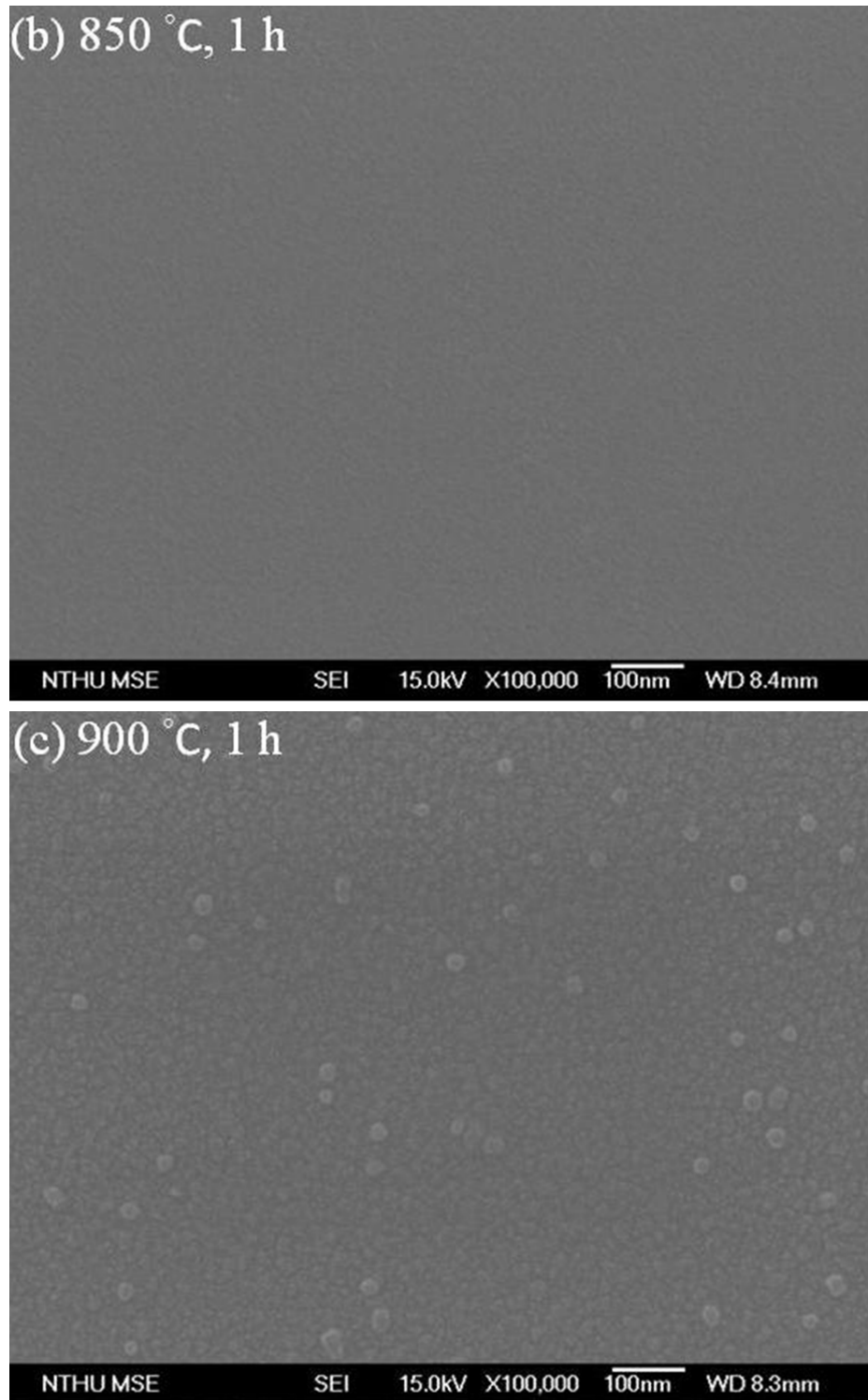


Figure 2. FE-SEM images of (a) as-deposited, (b) 850 °C-annealed and (c) 900 °C-annealed alloy thin films.

3. AFM analyses on as-deposited and as-annealed films

Figure 3 shows the AFM analyses of as-deposited (denoted as RT), 850 °C-annealed and 900 °C-annealed alloy thin films, including 3D images and RMS values. The surface roughness (RMS value) of 850 °C-annealed film is slightly smaller than that of the RT one. However, surface roughness of 900 °C-annealed alloy film is evidently larger than the RT one. This variation of roughness with annealing temperature is consistent with that observed with FE-SEM.

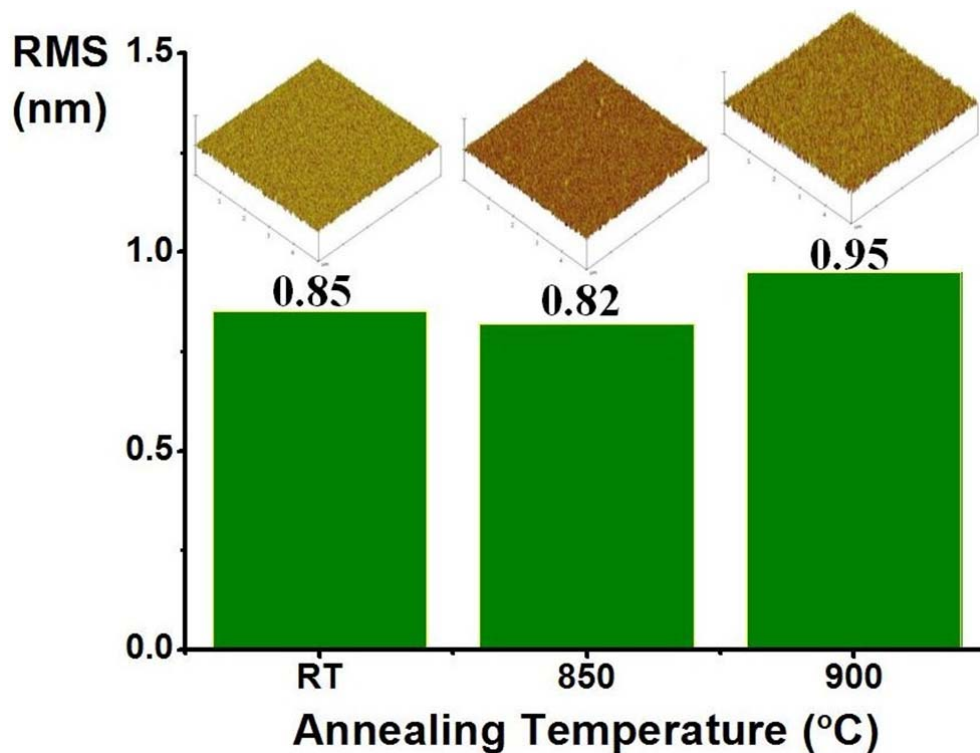


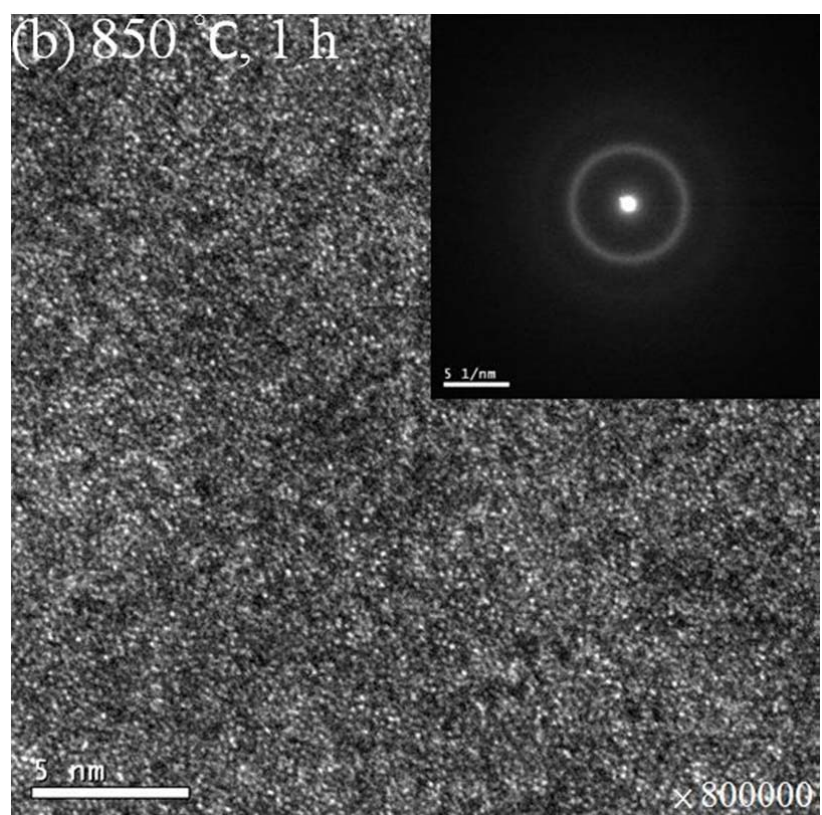
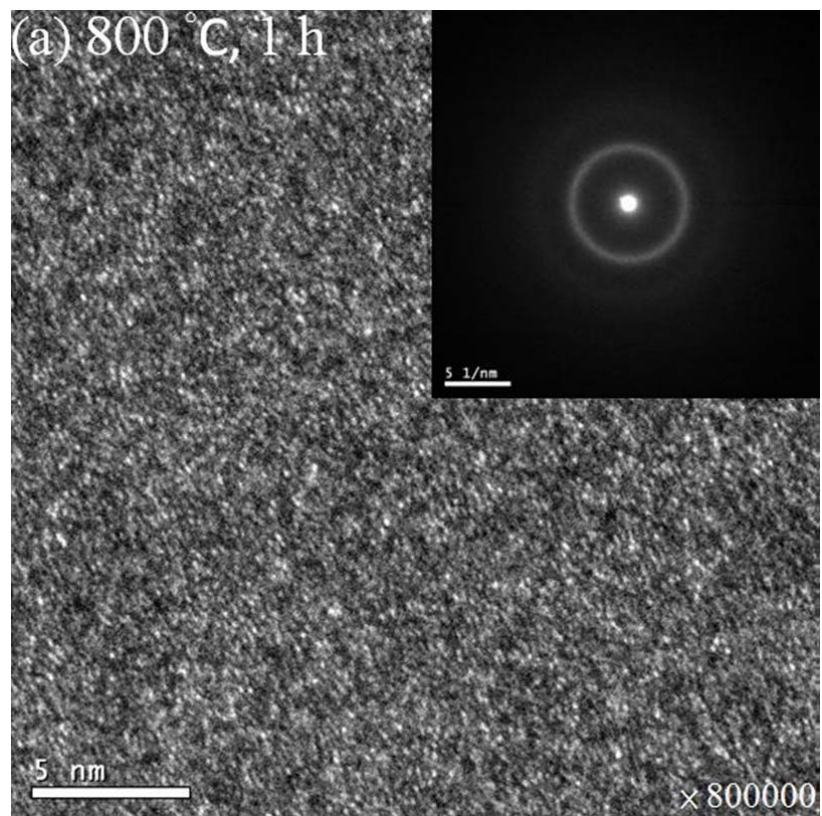
Figure 3. AFM analyses of as-deposited (denoted as RT), 850 °C-annealed and 900 °C-annealed alloy thin films.

4. TEM investigation on as-deposited and as-annealed films

Up to now, we can comprehend two important facts based on the results presented by XRD, SEM, and AFM analyses, as shown in Figure 1, 2, and 3. First, NbSiTaTiZr alloy thin films can sustain the amorphous structure after subjecting to rapid thermal vacuum annealing at 850 °C for 1 h (XRD: single diffuse peak, SEM: even surface

morphology, AFM: nearly same surface roughness) . Second, it might be conjectured that NbSiTaTiZr alloy thin films commence to crystallize under vacuum annealing at 900 °C for 1 h and form precipitates in the amorphous matrix. Although we've already known the above outcomes from XRD, SEM and AFM analyses, both facts still have to be examined elaborately. As a consequence, further TEM analysis is compulsory to be performed.

Figure 4 presents high resolution bright field image and selected-area-diffraction (SAD) patterns of (a) 800 °C-, (b) 850 °C- and (c) 900 °C-annealed alloy thin films, respectively. Both high resolution images of 800 °C-annealed and 850 °C-annealed samples reveal typical uniform salt-and-pepper feature of fully amorphous structure. Furthermore, their SAD patterns exhibit diffused rings. This again confirms that this coating can retain its amorphous structure after annealing at 800 °C and 850 °C for 1 h. Nevertheless, not only high resolution image but also SAD pattern illustrates that there are some crystallites dispersed in the amorphous matrix of 900 °C-annealed sample.



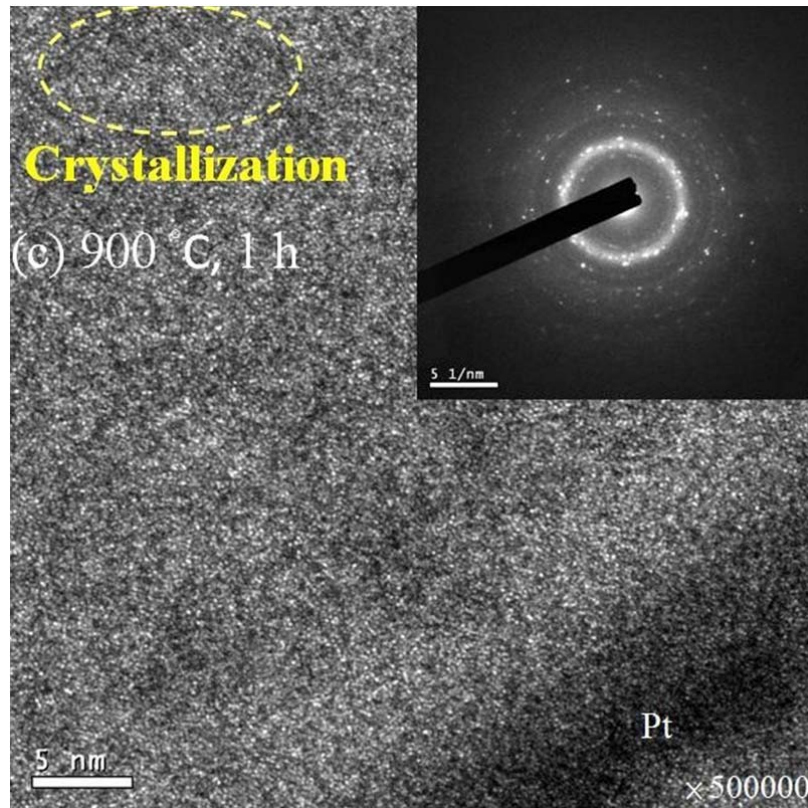


Figure 4. High resolution bright field image and selected-area-diffraction patterns of (a) 800 °C-, (b) 850 °C- and (c) 900 °C-annealed alloy thin films.

5. Substrate effect

For the crystallization phenomenon at 900 °C vacuum annealing, we propose that diffusion and chemical reaction have occurred during annealing treatment. It is well known that the formation energy of Zr oxide is very close to that of Al oxide. Thus, it is expected that Al₂O₃ near the interface are reduced by constituent elements Zr in thin film and the reduced Al atoms will diffuse into films to mix with other metals. In accompany with this, oxygen atom or ion will diffuse from Al₂O₃ substrate into the film to form other oxides, mainly Zr oxide. As a result, the chemical composition of affected diffusion zone and in turn was changed and the stability of amorphous structure of the films was reduced.

6. Strategy of alloy design for unusual thermal stable amorphous structure

If we compare the present crystallization temperature 850 °C with the reported crystallization temperatures of BMGs as listed in Tables 3, a large improvement of 323 °C is seen as compared to $\text{Ti}_{50}\text{Ni}_{20}\text{Cu}_{20}\text{B}_1\text{Si}_2\text{Sn}_3$ BMG with the highest crystallization temperature. It is generally believed that amorphous structure is unstable and tends to form crystalline structure in order to lower total free energy. This is primarily based on the fact that amorphous structure has lower coordination number in atomic configuration and higher distortion than crystalline structure. However, the present study demonstrates that this might not be true in high-entropy alloys. A suitable design such as the present NbSiTaTiZr alloy could have both high mixing entropy and large atomic size difference. This strategy not only uses high mixing entropy to enhance the solution state but also uses large atomic size difference (fulfilling the Inoue's second rule) to prevent crystallization at high temperatures.

Table 3. Thermal properties of various BMGs from reference [4]

BMG	T_g (K)	T_x (K)	T_m (K)	T_{fg}
Mg ₆₀ Ni ₁₀ Nd ₃₀	454.2	477.7	725.8	0.63
Mg ₆₅ Ni ₂₀ Nd ₁₅	459.3	501.4	743.0	0.62
Mg ₇₅ Ni ₁₅ Nd ₁₀	450.0	482.8	717.0	0.63
Mg ₇₀ Ni ₁₅ Nd ₁₅	467.1	494.1	742.5	0.63
Mg ₆₅ Cu ₂₅ Y ₁₀	424.5	484.0	727.9	0.58
Zr _{41.2} Ti _{13.8} Cu _{12.5} Ni ₁₀ Be _{22.5}	623.0	705.0	932.0	0.67
Zr _{46.75} Ti _{8.25} Cu _{7.5} Ni ₁₀ Be _{27.5}	622.0	727.0	909.0	0.68
Zr _{45.38} Ti _{9.62} Cu _{8.75} Ni ₁₀ Be _{26.25}	623.0	740.0	911.0	0.68
Zr _{42.63} Ti _{12.37} Cu _{11.25} Ni ₁₀ Be _{23.75}	623.0	712.0	933.0	0.67
Zr ₄₄ Ti ₁₁ Cu ₁₀ Ni ₁₀ Be ₂₅	625.0	739.0	917.0	0.68
Zr _{38.5} Ti _{16.5} Ni _{9.75} Cu _{15.25} Be ₂₀	630.0	678.0	921.0	0.68
Zr ₄₈ Nb ₈ Cu ₁₂ Fe ₈ Be ₂₄	658	751	1009	0.65
Zr ₄₈ Nb ₈ Cu ₁₄ Ni ₁₂ Be ₁₈	656	724	997	0.66
Zr ₅₇ Ti ₅ Al ₁₀ Cu ₂₀ Ni ₈	676.7	725.4	1095.3	0.62
Zr ₅₇ Nb ₅ Cu ₁₅ Al _{12.6} Al ₁₀	687	751	1092	0.63
Zr ₅₃ Ti ₅ Cu ₁₆ Ni ₁₀ Al ₁₆	697	793	1118	0.62
Zr ₆₆ Al ₉ Cu ₇ Ni ₁₉	662.3	720.7	1117.3	0.59
Zr ₆₆ Al ₉ Cu ₁₂ Ni ₁₄	655.1	732.5	1109.1	0.59
Zr ₆₆ Al ₉ Cu ₁₆ Ni ₉	657.2	736.7	1110.9	0.59
Zr ₆₆ Al ₉ Ni ₂₆	672.0	707.6	1188.5	0.57
Zr ₆₅ Al _{7.5} Cu _{17.5} Ni ₁₀	656.5	735.6	1108.6	0.59
Pd ₄₀ Ni ₄₀ P ₂₀	590.0	671.0	877.3	0.67
Pd _{81.5} Cu ₂ Si _{16.5}	633.0	670.0	1008.8	0.63
Pd ₄₀ Cu ₃₀ Ni ₁₀ P ₂₀	586.0	678.0	744.8	0.79
Pd _{42.5} Cu ₃₀ Ni _{7.5} P ₂₀	574.0	660.0	808.0	0.71
Pd _{77.5} Cu ₆ Si _{16.5}	637.0	678.0	1019.4	0.62
Pd _{42.5} Cu _{27.5} Ni ₁₀ P ₂₀	572.0	666.0	752.0	0.76
Cu ₆₀ Zr ₃₀ Ti ₁₀	713.0	763.0	1110.0	0.64
Cu ₅₄ Zr ₂₇ Ti ₉ Be ₁₀	720.0	762.0	1090.0	0.66
Cu ₆₀ Zr ₂₀ Hf ₁₀ Ti ₁₀	754	797	1189	0.63
La ₆₆ Al ₁₄ Cu ₂₀	395.0	449.0	681.9	0.58
La ₅₅ Al ₂₅ Ni ₂₀	490.8	555.1	711.6	0.69
La ₅₅ Al ₂₅ Ni ₁₀ Cu ₁₀	467.4	547.2	662.1	0.71
La ₅₅ Al ₂₅ Cu ₂₀	455.9	494.8	672.1	0.68
La ₅₅ Al ₂₅ Ni ₅ Cu ₁₀ Co ₅	465.2	541.8	660.9	0.70
Nd ₆₀ Al ₁₀ Cu ₁₀ Fe ₂₀	485.0	610.0	773.0	0.63
Nd ₆₀ Al ₁₅ Ni ₁₀ Cu ₁₀ Fe ₅	430.0	475.0	709.0	0.61
Nd ₆₁ Al ₁₁ Ni ₄ Co ₅ Cu ₁₅	445.0	469.0	729.0	0.61
Tb ₄ Zr ₁₁ Cu ₄₇ Ni ₈	698.4	727.2	1119.0	0.62
Ti ₅₀ Ni ₂₄ Cu ₂₀ B ₁ Si ₂ Sn ₃	726.0	800.0	1230.0	0.59
Au _{77.3} Si _{8.4} Ge _{13.3}	293.0	293.0	606.0	0.48
Pr ₆₀ Cu ₂₀ Ni ₁₀ Al ₁₀	409	452	705	0.58
Pr ₅₅ Al ₁₂ Fe ₃₀ Cu ₃	551	626	845	0.65

Most of data were obtained by DSC or/and DTA at a heating rate of 20 K/min.

IV. Conclusions

1. As-deposited NbSiTaTiZr alloy films are fully amorphous.
2. Annealing of the amorphous NbSiTaTiZr films at 850 °C for at least 3 h does not cause crystallization based on XRD, SEM and TEM analyses. However, annealing at 900 °C for 1 h causes some crystallization.
3. The devitrification phenomenon is due to the substrate effect. The interface reaction causes O ions and reduced Al atoms diffuse into the film and change the original chemical composition to enhance the crystallization.
4. Apart from the substrate effect, the amorphous structure of NbSiTaTiZr films

is very stable. The unusual stability is based on two combined effects from high entropy and sufficiently large atomic size difference.

V. References

- [1] A. Inoue, "Bulk amorphous and nanocrystalline alloys with high functional properties", *Materials Science and Engineering A*, 304-306 (2001) 1-10.
- [2] A. Inoue, W. Zhang, T. Zhang and K. Kurosaka, High-strength Cu-based bulk glassy alloys in Cu-Zr-Ti and Cu-Hf-Ti ternary systems, *Acta Materialia*, 49 (2001) 2645-2652.
- [3] A. Inoue and A. Takeuchi, "Recent progress in bulk glassy, nanoquasicrystalline and nanocrystalline alloys", *Materials Science and Engineering A*, 375-377 (2004) 16-30.
- [4] W. H. Wang, C. Dong, and C. H. Shek, "Bulk metallic glasses", *Materials Science and Engineering R*, 44 (2004) 45-89.
- [5] C. W. Chu, J. S. C. Jang, G. J. Chen, S. M. Chiu, "Characteristic studies on the Zr-based metallic glass thin film fabricated by magnetron sputtering process", *Surface and Coatings Technology*, 202 (2008) 5564-5566.
- [6] X. -Y. Li, E. Akiyama, H. Habazaki, A. Kawashima, K. Asami, and K. Hashimoto, "Electrochemical and XPS studies of the corrosion behavior of sputter-deposited amorphous Fe-Cr-Ni-Nb alloys in 6M HCl", *Corrosion Science*, 41 (1999) 1095-1118.
- [7] S. J. Pang, T. Zhang, K. Asami, A. Inoue, "Bulk glassy Fe-Cr-Mo-C-B alloys with high corrosion resistance", *Corrosion Science*, 44 (2002) 1847-1856.

- [8] S. J. Pang, T. Zhang, K. Asami, A. Inoue, "Bulk glassy Ni(Co-)Nb-Ti-Zr alloys with high corrosion resistance and high strength", *Materials Science and Engineering A*, 375-377 (2004) 368-371.
- [9] D. Zander, B. Heisterkamp, I. Gallino, "Corrosion resistance of Cu-Zr-Al-Y and Zr-Cu-Ni-Al-Nb bulk metallic glasses", *Journal of Alloys and Compounds*, 434-435 (2007) 234-236.
- [10] M. K. Tam, S. J. Pang, C. H. Shek, "Corrosion behavior and glass-forming ability of Cu-Zr-Al-Nb alloys", *Journal of Non-Crystalline Solids*, 353 (2007) 3596-3599.
- [11] H. M. Lin, J. K. Wu, C. C. Wang, P. Y. Lee, "The corrosion behavior of mechanically alloyed of Cu-Zr-Ti bulk metallic glasses", *Materials Letters*, 62 (2008) 2995-2998.
- [12] X. P. Nie, X. M. Xu, Q. K. Jiang, L. Y. Chen, Y. Xu, Y. Z. Fang, G. Q. Xie, M. F. Luo, F. M. Wu, X. D. Wang, Q. P. Cao and J. Z. Jiang, "Effect of microalloying of Nb on corrosion resistance and thermal stability of ZrCu-based bulk metallic glasses", *Journal of Non-Crystalline Solids*, 355 (2009) 203-207.
- [13] C. L. Qin, W. Zhang, Q. S. Zhang, K. Asami, A. Inoue, "Electrochemical properties and surface analysis of Cu-Zr-Ag-Al-Nb bulk metallic glasses", *Journal of Alloys and Compounds*, 483 (2009) 317-320.
- [14] C. L. Qin, Y. Q. Zeng, D. V. Louzguine, N. Nishiyama, A. Inoue, "Corrosion resistance and XPS studies of Ni-rich Ni-Pd-P-B bulk glassy alloys", *Journal of Alloys and Compounds*, S504 (2010) S172-S175.
- [15] W. H. Wang, "Bulk metallic glasses with functional physical properties",

- Advanced Materials, 21 (2009) 4524-4544.
- [16] A. Inoue, "Stabilization of metallic supercooled liquid and bulk amorphous alloys", *Acta Materialia*, 48 (2000) 279-306.
- [17] A. Inoue, X. M. Wang and W. Zhang, Developments and applications of bulk metallic glasses, *Reviews on Advanced Materials Science*, 18 (2008) 1-9.
- [18] J. C. Huang, J. P. Chu, J. S. C. Jang, "Recent progress in metallic glasses in Taiwan", *Intermetallics*, 17 (2009) 973-987.
- [19] A. Inoue and A. Takeuchi, "Recent development and application products of bulk glassy alloys", *Acta Materialia*, 59 (2011) 2243-2267.
- [20] H. S. Chen, *Metallic Glasses*, *Chinese Journal of Physics*, 28 (1990) 407-425.
- [21] G. Duan, A. Wiest, M. L. Lind, J. Li, W. K. Rhim, W. L. Johnson, "Bulk metallic glass with benchmark thermoplastic processability", *Advanced Materials*, 19 (2007) 4272-4275.